one case, A_{In} = 4.85, implying an indium(III) species, and coupling constants were assigned for each pair of hydrogen atoms of the phenanthrene ring, with values essentially independent of the halide involved. It was not possible to assign values for the indium(I) analogue.

The number of hyperfine constants in this system does not allow for a detailed analysis of the species present in this solution, but the results can be summarized in Scheme II, which invokes a series of reactions which proceed by one-electron transfer. The detailed differences between the TBQ and PQ systems are presumably the result of the differing oxidizing potentials, and/or steric effects, in the two series of compounds.

Discussion

The present work, and earlier studies from this department,[9-11] shows that the oxidation of indium(I) to indium(III), or of tin(II) to tin(IV), by *o*-quinones is not a one-step two-electron transfer process. It has frequently been assumed in discussions of redox reactions in main group chemistry that because the oxidation states identified under normal conditions differ by two electrons, the intermediate states such as tin(III) and indium(II) have no relevance to the overall chemistry of these elements. The fact that most redox reactions in solutions of main group compounds are rapid has hindered any detailed investigation of these processes and has led to the conclusion, in the absence of evidence to the contrary, that two-electron transfers are the norm. The present investigations, involving oxidizing agents in which the successive electron addition processes can be identified spectroscopically, show that one-electron transfer reactions may well be as significant with main group compounds as they are in the more thoroughly studied transition element field. Work on related systems is continuing.

Acknowledgment. This work was supported in part by Operating Grants (to B.R.M. and D.G.T.) from the Natural Sciences and Engineering Research Council of Canada.

Supplementary Material Available: Tables of refined anisotropic thermal parameters and fractional coordinates and thermal parameters for hydrogen atoms and cell packing diagram (4 pages); a table of observed and calculated structure factors (11 pages). Ordering information is given on any current masthead page.

Contribution from the Department of Chemistry and Materials Science Center, Cornell University, Ithaca, New York 14853-1301

Electronic and Structural Properties of the Novel Chain Compound Ta_4Te_4Si

Jing Li, Roald Hoffmann,* Michael E. Badding, and Francis J. DiSalvo

Received November 21, 1989

Some interesting aspects of the newly synthesized chain structure Ta_4Te_4Si are discussed in this paper. A fragment analysis shows that both metal-metal bonding and Ta-Si bonding are strong and are responsible for the stabilization of the chain. Band structure calculations suggest that the compound is a metallic conductor. The states that contribute to the conduction bands are derived mostly from the Ta 5d orbitals. The relative stabilities of different structural choices are compared, and possible geometrical distortions are examined. It should be possible to replace the interstitial Si by transition metals, especially Fe or Co. Finally, we examine the possibility of oxidation and reduction of the chain.

Introduction

Molybdenum chalcogenide cluster compounds (e.g., the Chevrel phases)[1] have received much attention from both chemists and physicists, due to their many interesting structural, chemical, and physical properties.[2] These include superconductivity, magnetic ordering at low temperatures, charge density waves, and some anisotropic behavior.[3] In an attempt to make tantalum and niobium ternary phases of the molybdenum analogue, Badding and DiSalvo have recently synthesized a new chain compound, Ta_4Te_4Si, whose single-crystal has been determined by X-ray diffraction techniques.[4] One view of the structure is shown in Figure 1. The basic building unit of this novel material is the square-pyramidal Ta_4Si (**1**) with Ta atoms bridged by telluriums

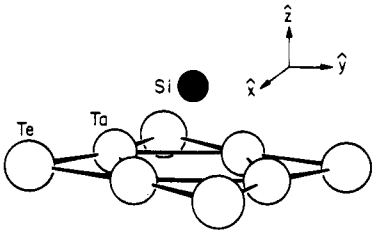

1

in the same (*xy*) plane. Such units stack along the *c* axis in an antiprismatic fashion and form an infinite chain. The chain–chain separation is large, giving a closest Te–Te contact of 3.815 Å. Structurally, this compound is closely related to the binary Ta_2S[5] and the ternary $InMo_3Te_3$,[6] which also contain antiprismatically arranged metal chains: pentagonal and trigonal, respectively. The Si atoms in this compound sit in the center of each square antiprism, forming a nearly equally spaced single-atom chain along the *c* axis. The situation is similar to what has been observed in another metal-rich ternary tantalum chalcogenide, $Ni_2Ta_9S_6$,[7] where the Ni atoms in the centers of trigonal prisms formed by six Ta atoms generate an entirely symmetric chain.

Recent synthetic experiments indicate that the central Si atoms may be replaceable by other elements, such as the main-group

(1) Chevrel, R.; Sergent, M.; Prigent, J. *J. Solid State Chem.* **1971**, *3*, 515.
(2) See, for example: Lawson, A. C. *Mater. Res. Bull.* **1972**, *7*, 773. Sergent, M.; Chevrel, R. *J. Solid State Chem.* **1973**, *6*, 433. Morton, N.; Booth, J. G.; Woodhead, C. F. *J. Less-Common Met.* **1974**, *34*, 12. Bader, S. D.; Knapp, G. S.; Sinha, S. K.; Schweiss, P.; Renker, B. *Phys. Rev. Lett.* **1976**, *37*, 344. Kimball, C. W.; Weber, L.; van Landuyt, G.; Fradin, F. Y.; Dunlap, D. B.; Shenoy, G. K. *Phys. Rev. Lett.* **1976**, *36*, 412. Yvon, K.; Paoli, A.; Fükiger, R.; Chevrel, R. *Acta Crystallogr.* **1977**, *B33*, 3066. Johnson, D. C.; Shelton, R. N. *J. Low Temp. Phys.* **1977**, *26*, 561. Hönle, W.; Yvon, K. *J. Solid State Chem.* **1987**, *70*, 235.
(3) Marezio, M.; Dernier, P. D.; Remeika, J. P.; Corenzwit, E.; Matthias, B. T. *Mater. Res. Bull.* **1973**, *8*, 657. Alekseevskii, N. E.; Dobrovolskii, N. M.; Tsebro, V. I. *JETP Lett.* **1976**, *23*, 639. Shelton, R. N.; McCallum, R. W.; Adrian, H. *Phys. Lett.* **1976**, *56A*, 213. Pelizzone, M.; Treyvaud, A.; Spitzli, P.; Fischer, Ø. *J. Low Temp. Phys.* **1977**, *29*, 453. Fischer, Ø. *Appl. Phys.* **1978**, *16*, 1.
(4) Badding, M. E.; DiSalvo, F. J. *Inorg. Chem.*, following paper in this issue.
(5) Franzen, H. F.; Smeggil, J. G. *Acta Cryst.* **1969**, *B25*, 1736.
(6) Hönle, W.; von Schnering, H. G.; Lipka, A.; Yvon, K. *J. Less-Common Met.* **1980**, *71*, 135.
(7) Harbrecht, B.; Franzen, H. F. *J. Less*-Common *Met.* **1986**, *115*, 177. Herbercht, B. *J. Less-Common Met.* **1986**, *124*, 125.

0020-1669/90/1329-3943$02.50/0

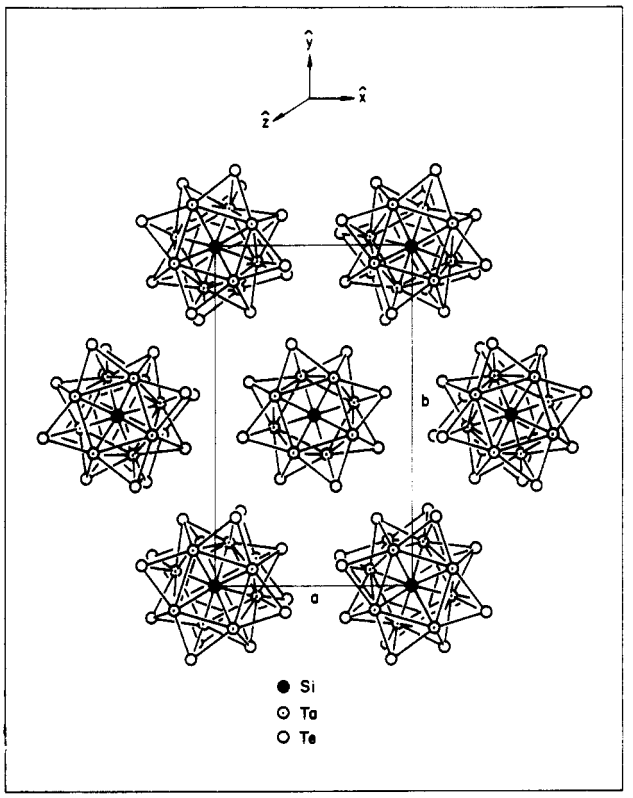

Figure 1. Perspective view of the Ta_4Te_4Si structure along the z direction (c axis). The open circles are the Te atoms, and the solid circles, the Si atoms. Ta atoms are labeled by open circles with a dot in the center.

Al and transition-metal Cr, Fe, Co, and Ni. With tight-binding band calculations[8] of the extended Hückel type,[9] we would like to explore, in the present study, some interesting aspects of this novel chain compound, in particular the structural preferences, the electrical conductivity, the possibility of dimerization, and the introduction of other atoms into the Si site. A detailed description of the computations and the atomic parameters are listed in the Appendix.

Description of the Chain Structure

The compound under consideration belongs to space group *Pbam* of the orthorhombic system, with its lattice constants being 10.54, 18.28, and 4.80 Å, respectively. A perspective view of this structure along the c axis was shown in Figure 1, where the unit cell is highlighted. The Ta_4Te_4Si monomer stacks antiprismatically along the z direction (c axis), **2**, to form an infinite chain as

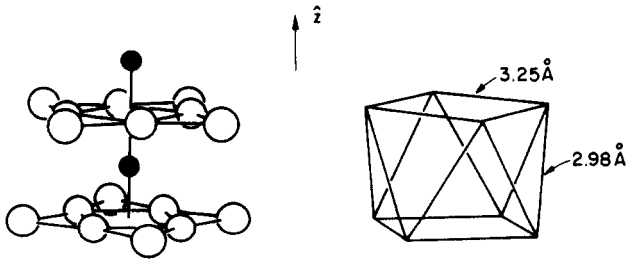

2

sketched in **3** (only Ta and Si atoms are shown for clarity). The intersquare and intrasquare Ta–Ta distances are 2.98 and 3.25

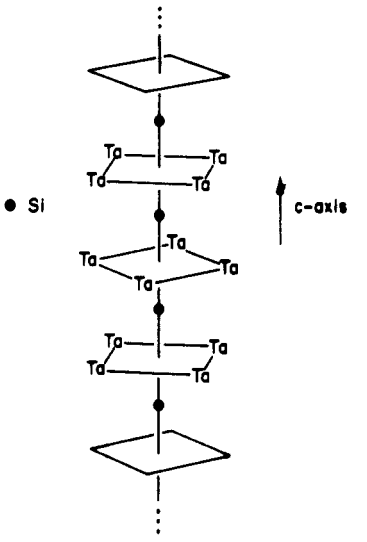

3

Å (average value), respectively, as indicated in **2**. Compared to the Ta–Ta separation in the metal (bcc), 2.86 Å,[10] these are a little longer but certainly within bonding range. The Ta–Te bonds, 2.84 Å (intrasquare, average value) and 2.97 Å (intersquare, average value) are comparable to a Ta–Te bond length, 2.86 Å, derived from averaging the Ta–Ta and Te–Te distances in metals.[11] The Si atom, sitting in the center of the square antiprism, has a close contact with the eight tantalums at 2.59 Å (average value), as shown in **4**. It also bonds to two other silicons from the neighboring cells (2.448 and 2.353 Å), giving rise to a single atom chain parallel to the c axis, **5**.

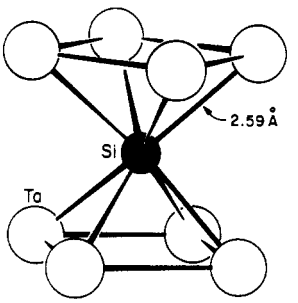

4

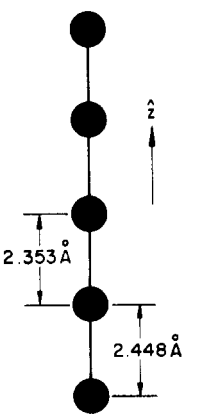

5

There are "channels" running between the Ta_4Te_4Si chains. One of these is outlined in **6**. As pointed out earlier, the shortest chain–chain separation is 3.815 Å, a distance characterized by

(8) Hoffmann, R.; Whangbo, M.-H. *J. Am. Chem. Soc.* **1978**, *100*, 6093. Whangbo, M.-H.; Hoffmann, R.; Woodward, R. B. *Proc. R. Soc. London* **1979**, *A366*, 23. Hoffmann, R. *Rev. Mod. Phys.* **1988**, *60*, 601. Hoffmann, R. *Solids and Surfaces: A Chemist's View of Bonding in Extended Structures*; VCH: New York, 1988.

(9) Hoffmann, R. *J. Chem. Phys.* **1963**, *39*, 1397. Hoffmann, R.; Lipscomb, W. N. *J. Chem. Phys.* **1962**, *36*, 2179, 3489; **1962**, *37*, 2872. Ammeter, J. H.; Burgi, H.-B.; Thibeault, J. C.; Hoffmann, R. *J. Am. Chem. Soc.* **1978**, *100*, 3686.

(10) Ashcroft, N. W.; Mermin, N. D. *Solid State Physics*; Holt, Rinehart and Winston: Philadelphia, PA, 1976.

(11) *Tables of Interatomic Distances and Configurations in Molecules and Ions*, Supplement, 1956–1959; Special Publication No. 18; Sutton, L. E., et al., Scientific Eds.; The Chemical Society: London, 1965.

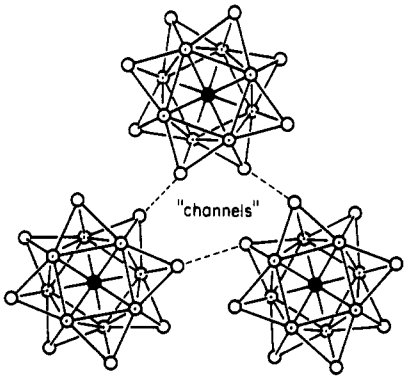

6

Te–Te van der Waals contact. The channels in the present structure are not as "open" as those in the $M_2Ta_9S_6$ structures or other metal tantalum sulfides.[12]

Electronic Properties of the Chain

To understand the bonding in the Ta_4Te_4Si chain, let us begin with construction of the orbital diagram of a monomer. Because the differences in the electronegativities of the component elements are not large, our working assumption is to use neutral fragments (Ta_4, Ta_4Te_4, and Ta_8Te_8Si) as we build up the polymer. Figure 2 shows what happens to the Ta 5d orbitals when the four atoms approach to form a square-planar Ta_4 fragment. These orbitals are most responsible for the metal–metal bonding and will be the major participants in the Ta–Te and Ta–Si bonding to be discussed. In the lower portion of the diagram is a block of bonding orbitals, numbered 1–7. We see typical bonding interactions of all kinds: σ, π, and δ. Correspondingly, the seven antibonding orbitals appear in the upper part of the diagram. These are numbered 14–20. The six remaining nonbonding orbitals are outlined in the central portion, where the highest occupied orbitals (HOMO) for a neutrai Ta_4 species are located. The result is net metal–metal bonding. An overlap population of 0.367 for each Ta–Ta bond is computed. It is clear that removing electrons (oxidation) would enhance the bonding whereas adding electrons (reduction) would diminish such bonding.

The interactions between the square-planar Ta_4 (5d orbitals) and the Te ligands are shown schematically in Figure 3. On the left are the Ta_4 orbitals, partitioned from bottom up into bonding, nonbonding, and antibonding sets. The Te 5s and 5p orbitals are those at right. The resultant MO's are shown in the central portion of the diagram in the form of blocks. Strong Ta–Te bonds (overlap population = 0.67) are obtained in the Ta_4Te_4 species. The Te 5p's contribute significantly to the Ta–Te bonding orbitals and are stabilized, whereas the antibonding orbitals are derived mainly from Ta 5d antibonding combinations. Inbetween is the region of metal-based orbitals, Ta–Ta bonding, nonbonding, and antibonding. A few of these are depicted in **7**. These are the Ta orbitals particularly well set up for intersquare Ta–Ta bonding and Ta–Si bonding, to which we now turn.

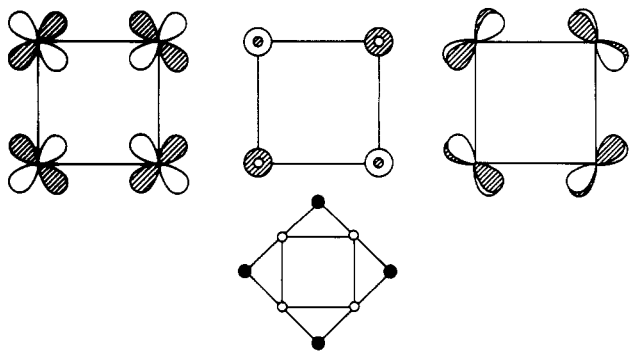

7

(12) Schlögl, R.; Bensch, W. *J. Less-Common Met.* **1987**, *132*, 155. Reference 5.

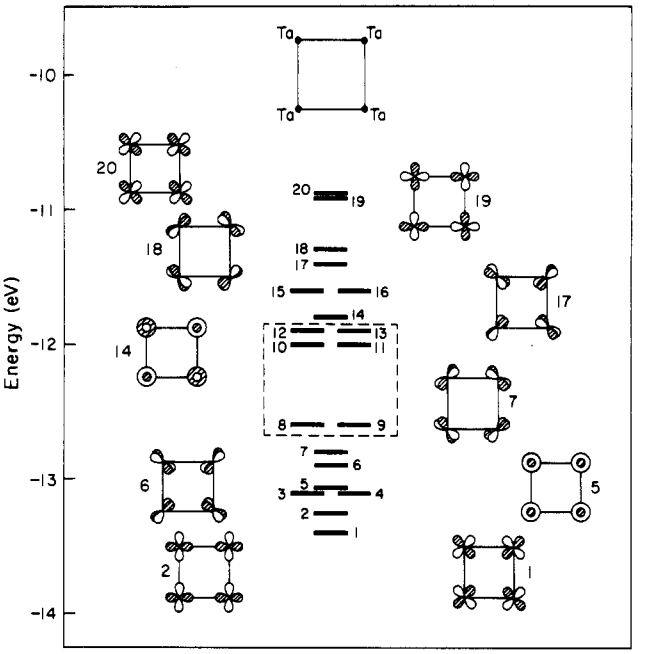

Figure 2. Schematic orbital interaction diagram for a square-planar Ta_4 fragment. Only those orbitals resulting from the Ta 5d interactions are drawn. The nonbonding orbitals are outlined.

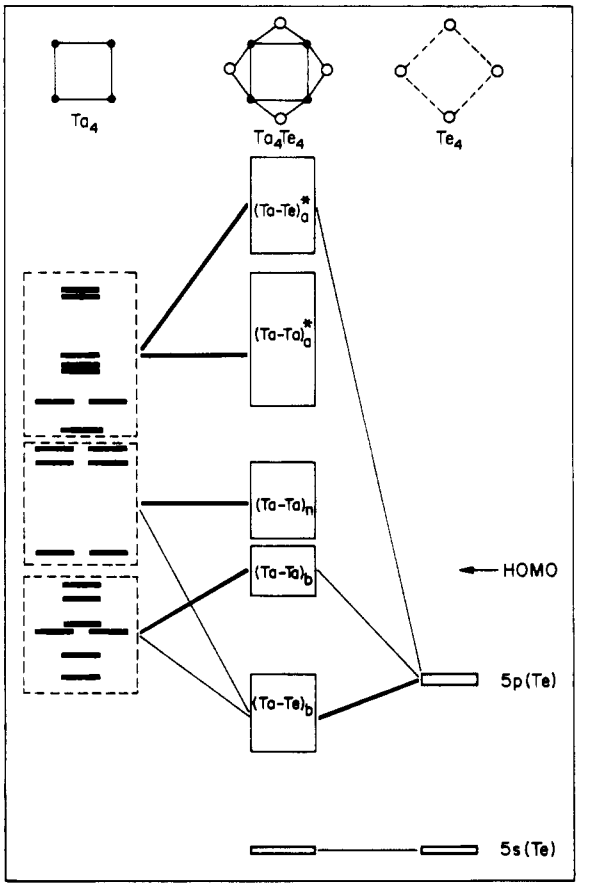

Figure 3. Orbital interaction scheme (in block form) for Ta_4 and Te_4 species. The HOMO (highest occupied molecular orbital) is indicated in the figure by an arrow.

As one stacks a Ta_4 unit over another rotated 45° about the c axis, the intersquare interactions are turned on. The main states contributing to Ta–Ta′ (intersquare Ta–Ta) bonding, denoted as $(Ta\text{–}Ta')_b$ in **8**, are also Ta–Ta (intrasquare Ta–Ta) bonding, $(Ta\text{–}Ta)_b$. On the other hand, the Ta–Ta′ antibonding states, $(Ta\text{–}Ta')_a^*$, have great Ta–Ta antibonding character. The states inbetween are a mixture of all possible combinations.

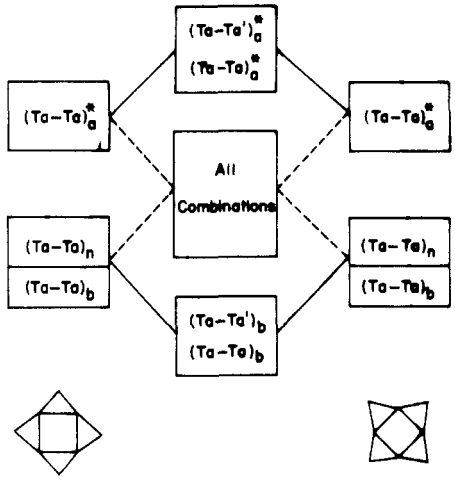

8

A model study of Ta_8Si reveals that the Ta–Si bonding is localized to a small energy interval (see Figure 4). The energy dispersion of the Ta–Si bonding orbitals is small and is confined to a window of ~1.6 eV. The metal cluster orbitals most responsible for the bonding are $1b_1$, $2b_2$, and e_1, which interact strongly with the Si $3p_z$ and $3p_x + 3p_y$, respectively. Perhaps it helps to look at the cartoon in **9**, where one bonding orbital resulted mainly from $2b_2$ and Si $3p_z$ interacting is drawn.

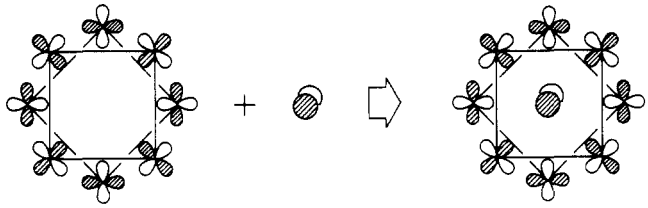

9

The molecular orbital picture constructed above serves as a tool for understanding the electronic structure of the infinite chain. There are many resemblances. The fragment analysis[13] is employed here, as earlier. The fragments are now a single atom chain, $(Si)_\infty$ (**10a**), and the Ta_4Te_4 sublattice (**10b**). Important overlap

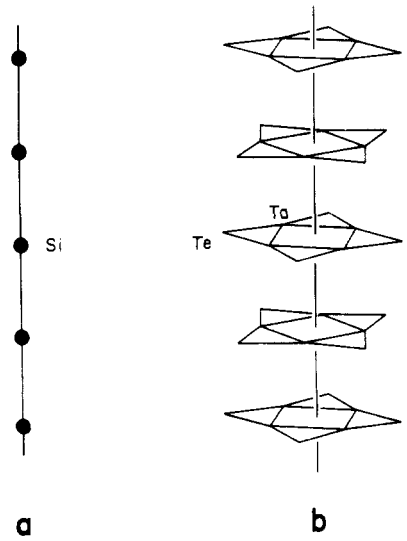

10

populations calculated for these fragments and the composite system are compared in Table I. Let us focus first on the results from the fragments or sublattices. These are listed in the first

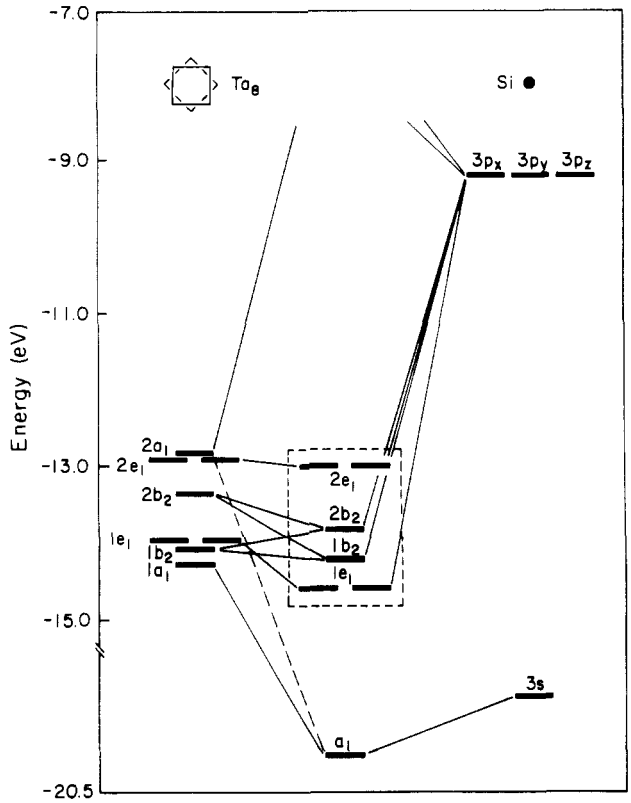

Figure 4. Schematic diagram showing the interactions between a Si atom and a Ta_8 fragment in a geometrical arrangement as depicted in **4**.

Table I. Overlap Populations for the Two Sublattices (Ta_4Te_4 and Si Chain) and the Composite System Ta_4Te_4Si Chain

	OP[a]		
	$(Ta_4Te_4)_\infty$ or $(Si)_\infty$	$(Ta_4Te_4Si)_\infty$	Δ(OP)
Ta–Ta	0.249	0.156	−0.093
Ta–Ta′	0.343	0.288	−0.055
Ta–Te	0.435	0.437	0.003
Ta–Te′	0.407	0.396	−0.011
Si–Si	1.162	0.280	−0.882
Ta–Si		0.270	0.270

[a] OP = overlap populations.

column. The strong Ta–Ta, Ta–Ta′ bonding (0.249 and 0.343) are immediately noticed. The latter is stronger, as expected from the shorter intersquare bond length. With overlap population values of 0.435 and 0.407, respectively, the Ta–Te (intrasquare Ta–Te) bonding and Ta–Te′ (intersquare Ta–Te) bonding are also strong. Given an overlap population of 1.162, the Si–Si bond in a neutral Si chain is very strong. This value represents the maximum bonding possible in a Si–Si chain. Compared to the numbers in the second column, the most dramatic change occurs in the Si–Si bond (greatly decreased). New and strong Ta–Si bonds are formed. The Ta–Te interactions are little affected, but the Ta–Ta bonds, both intra- and intersquare, are weakened to some degree.

The bonding may be analyzed with the aid of densities of states (DOS),[14] their decompositions, and crystal orbital overlap populations (COOP).[15] Figure 5 shows some of these for Ta_4Te_4Si. The Ta–Si bonding comes mainly from Ta $5d_{xz}$, $5d_{yz}$ (left panel of the figure) and Si $3p_x$ and $3p_y$ (middle panel) interactions, which can be easily understood from DOS projections plotted at the bottom of Figure 5 (other Ta 5d orbitals, for example $5d_{z^2}$ and $5d_{x^2-y^2}$, also contribute to the Ta–Si bonding, but to a smaller extent). About half of the $5d_{xz}$, $5d_{yx}$ states of the subchain Ta_4Te_4

(13) Hoffmann, R.; Swenson, J. R.; Wan, C.-C. *J. Am. Chem. Soc.* **1973**, *95*, 7644. Fujimoto, H.; Hoffmann, R. *J. Phys. Chem.* **1974**, *78*, 1167.

(14) Hoffmann, R. *Angew. Chem.* **1987**, *99*, 871; *Angew. Chem., Int. Ed. Engl.* **1987**, *26*, 846.

(15) Hughbanks, T.; Hoffmann, R. *J. Am. Chem. Soc.* **1983**, *105*, 1150.

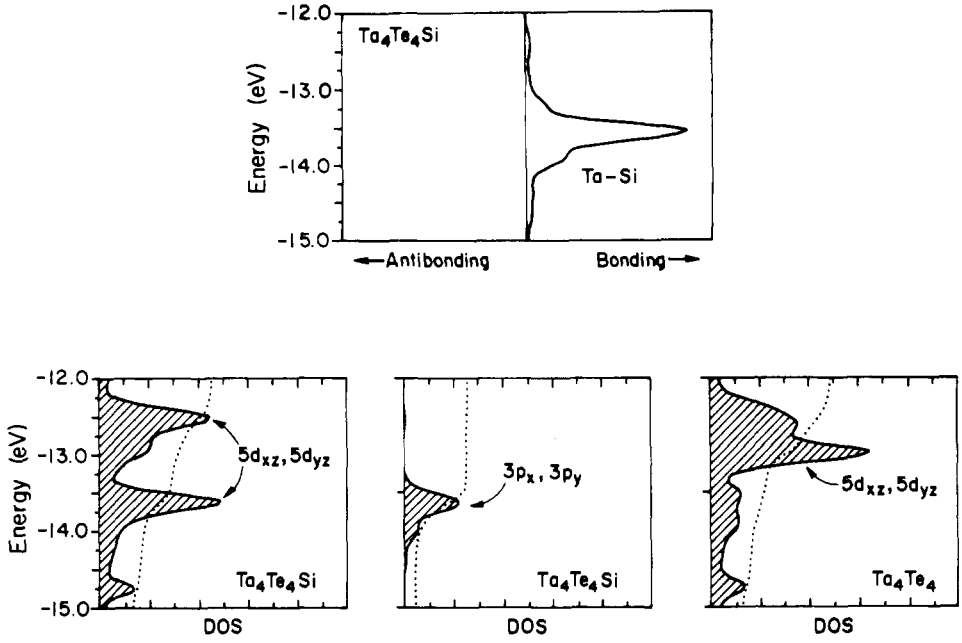

Figure 5. DOS (density of states) projections and the COOP (crystal orbital overlap population) curves for the chain systems. In the top panel is the COOP curve for the Ta-Si bond, and in the lower panels are DOS of the Ta $5d_{xz}$, $5d_{yz}$ (left), the Si $3p_x$, $3p_y$ (middle) of the Ta_4Te_4Si chain, and the Ta $5d_{xz}$, $5d_{yz}$ (right) of the Ta_4Te_4 subchain. The dotted lines give the integration of the projected orbitals (full scale = 100% occupation).

(right panel) are stabilized in the composite system; the original peak centered between −12.0 and −13.25 eV splits into two; while one remains in that region, the other is lowered to −13.25 to −14.0 eV. Most bonding states are within a narrow 1.0-eV energy region, as in the molecular case. The COOP curve, also plotted in Figure 5, clearly shows this.

A view of the Si–Si and Ta–Ta (both inter- and intrasquare bond) COOP curves in the subchains reveals that they also are all bonding within the −12- to −15-eV interval. What does this imply? For tantalum, some of these bonding orbitals, originally filled, will contribute in the Ta–Si antibonding region (empty) in the composite system. Thus weakening of the Ta–Ta bonds will result. But it will not be too great, since it is the Si states that participate mainly in the Ta–Si antibonding. The majority of the Ta states will be stabilized upon that interaction, as seen in **11**. For Si atoms, on the other hand, participation of their

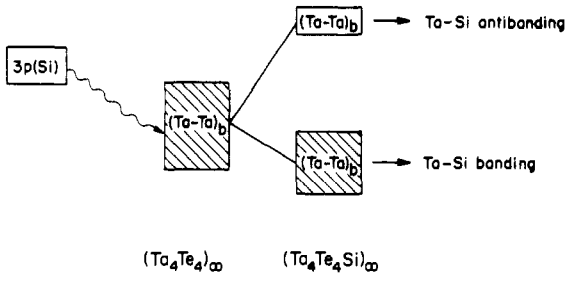

11

antibonding orbitals (originally empty) in the Ta–Si bonding (**12a**) and their bonding orbitals (originally filled) in the Ta–Si antibonding (**12b**) will cause a dramatic decrease in Si–Si overlap population.

Ta_4Te_4Si should be metallic. This follows from the calculated band structure plotted in Figure 6a. There are three bands near the Fermi level. Two of these (bands 44 and 49), both approximately half-filled, are primarily responsible for the conductivity of this chain. There are practically no Si contributions to these bands. This can be realized by comparing Figure 6a to Figure 6b; the latter is a band structure of the subchain Ta_4Te_4. The bands in the region of the Fermi level show remarkable resemblance to those in Figure 6a. Indeed, a simple computation of the percentage contribution of the three components of the total DOS in the energy interval between −11 and −12 eV gives the following: Ta, 78.2%; Te, 17.2%; Si, 4.6%.

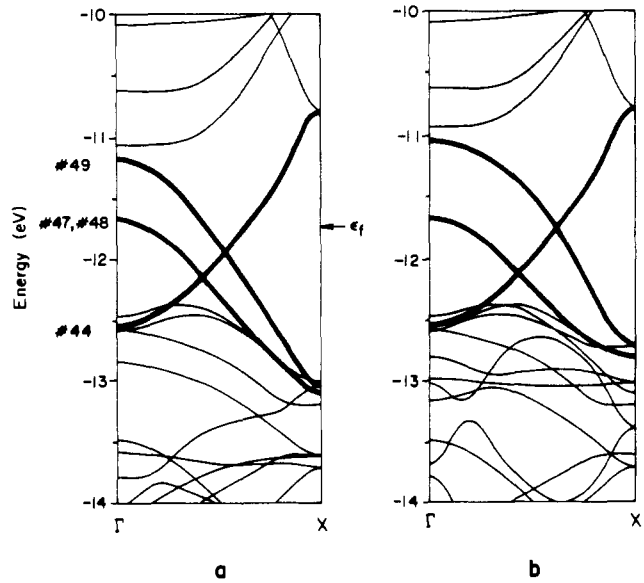

Figure 6. Band structure for the Ta_4Te_4Si chain (a), and for the Ta_4Te_4 subchain (b). Orbitals around the Fermi level ϵ_F (indicated with an arrow) are emphasized by heavy lines and are numbered in part a.

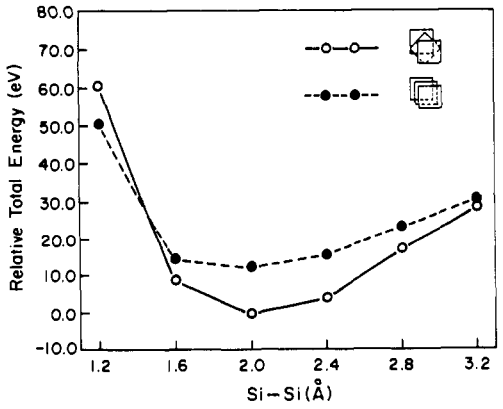

Figure 7. Relative average total energy per unit cell versus the Si–Si distance plotted for the staggered form (solid line) and the eclipsed form (dashed line).

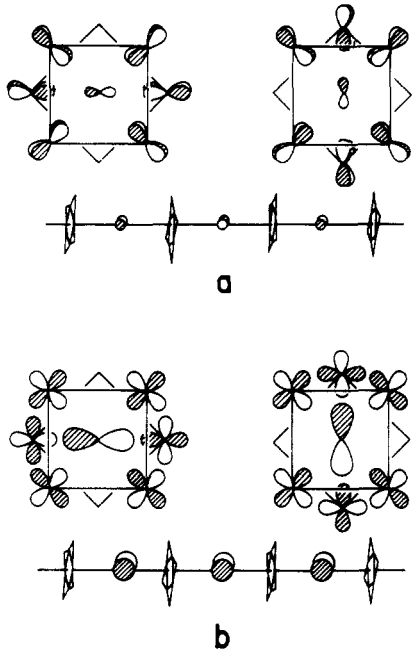

12

The experimental measurement of conductivity has proved difficult.[4] This difficulty is due to two factors: (1) The crystals are fragile due to the van der Waals bonding between the chains. They tend to form a fine fan of fibers when mechanically handled. (2) The compound is quite air-sensitive. Exposure to air seems to form an insulating layer on the crystal surface, which makes the formation of good electrical contacts difficult. Work is still in progress to unambiguously determine the electrical characteristics of this material.

A one-dimensional model for the Ta_4Te_4Si structure has been employed in all calculations discussed above. This approximation is based on the fact that the interchain interactions appear negligible. To confirm this, we have repeated our calculations with a three-dimensional model, including such interchain interactions. The result, not surprisingly, is very similar to that obtained for the 1D chain. The differences in the overlap population values are all within 0.008, and ϵ_F is the same to 0.01 eV. All the bands along ΓX and ΓY in the Brillouin zone (directions perpendicular to the chain axis) are very flat, with a maximum 0.5-eV dispersion from a band above the Fermi level.

Geometrical Choices of the Chain

The metal framework of Ta_4Te_4Si is built up by antiprismatically stacked Ta_4 squares. An alternative that comes to mind is **13**, in which the chain is formed by prismatically stacked Ta_4

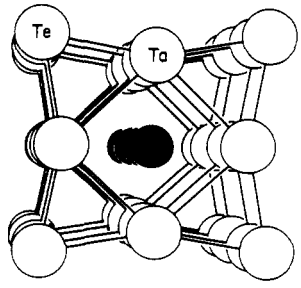

13

squares. The relation between the two structures is very much like that between staggered and eclipsed ethane (**14**). For this reason, we denote them as "staggered" and "eclipsed" as well. For ethane, it is known that the eclipsed conformer is less stable than the staggered one, due to repulsion between the C–H bonds.[16] In

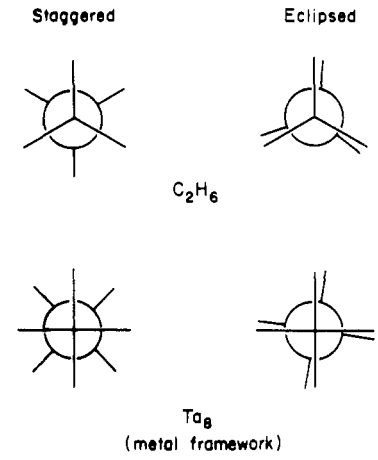

14

Ta_4Te_4Si, however, the situation is not so clear. Several interatomic distances are affected on going from the staggered to eclipsed isomer, and these always involve two atoms from two neighboring square units. If the Si–Si distance is kept at 2.4 Å, then the changes are listed as below: Ta–Ta′, 2.979 to 2.40 Å; Te–Te′, 3.87 to 2.40 Å; and Ta–Te′, 2.92 to 3.72 Å. As one moves from staggered to eclipsed, considerable increases in overlap populations are found for both intersquare Ta–Ta and Ta–Te bonds. At the same time, a great decrease for intersquare Ta–Te bonding is computed. The two opposing factors compete, and the latter wins. A stabilization of 11.1 eV for the staggered (square antiprism) Ta_4Te_4Si is obtained over the eclipsed (square prism) form. We have carried out a geometrical optimization as a function of the Si–Si separation. Figure 7 illustrates the result. For a reasonable range of Si–Si separations, the staggered conformer is always energetically more stable than the eclipsed one, consistent with the experimental observations. Notice that the energy minimum appears at a Si–Si distance of ~2.0 Å, deviating from the reported 2.4 Å (average value). This is not a surprise, since extended Hückel calculations are not very reliable for absolute bond lengths. Nevertheless, such calculations give a reasonable estimate of the shape of the energy curve versus bond lengths.

With a chain electronic structure that has one or more partially filled bands, a question immediately arises: Is there a potential for a structural deformation, a Peierls distortion?[17] In other words, will the system undergo a spontaneous geometrical change in which atoms dimerize, trimerize, or rearrange themselves to lower the DOS near the Fermi level?

For the Ta_4Te_4Si chain under study, we would like to see what are the consequences of such distortions. A careful view of its band structure (Figure 6a) reveals (a) that around the Fermi level there are two bands which are approximately half-filled (bands 44 and 49) with the third one, the degenerate bands 47 and 48, nearly completely filled and (b) that these two partially filled bands cross; i.e., they differ in symmetry. One way that we could think of to stabilize the chain is to lower the symmetry of the system so that these two bands become of the same symmetry. Then, an avoided crossing near the middle point of the Brillouin zone should occur. The situation would be similar to what is called a second-order Jahn–Teller effect[18] in a molecular complex, **15**, and the system would be stabilized.

A careful view of these bands shows that the difference in symmetry for the two is caused by symmetry operations *within* the *xy* plane. **16** tells why. Crystal orbitals (only drawn for a

(16) Lowe, J. P. *J. Am. Chem. Soc.* **1970**, *92*, 3799; **1974**, *96*, 3759.

(17) Peierls, R. E. *Quantum Theory of Solids*; Oxford University Press: London, 1955, p 108. Whangbo, M.-H. In *Crystal Chemistry and Properties of Materials with Quasi-One-Dimensional Structure*; Rouxel, J., Ed.; Reidel: Dordrecht, The Netherlands, 1986.

(18) Albright, T. A.; Burdett, J. K.; Whangbo, M.-H. *Orbital Interactions in Chemistry*; Wiley: New York, 1985.

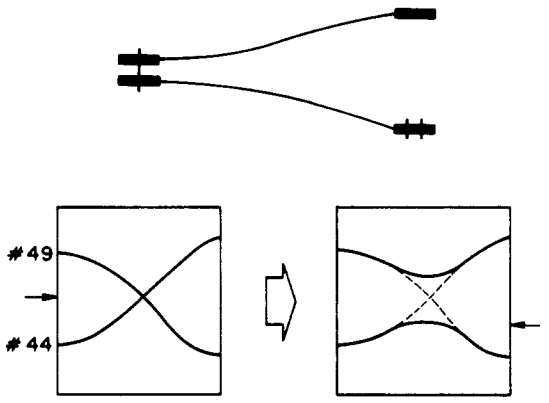

15

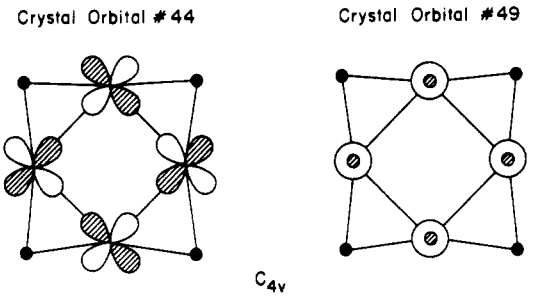

16

Ta_4 square unit) corresponding to the two bands under consideration at the zone center (Γ point) are shown. Carrying out the symmetry operations of a C_{4v} point group (those involving changes of the z components are ignored here) on orbital 44 allows us assign it readily to an A_2 representation, whereas orbital 49 is A_1. To make these two bands of the same symmetry type, the distortions must be such that they cause changes in the x and y components of the orbitals. One such deformation is shown in **17**. The

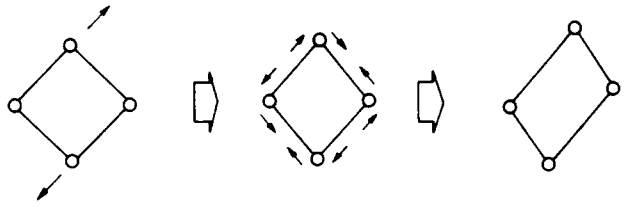

17

distortion changes the symmetry from C_{4v} into C_2. Under point group C_2, the two orbitals now belong to representation A. However, with the given experimental geometry, the deformation of this kind is too small to actually open a gap between the two bands. What, then, a distortion *along* the chain axis, for example pairing of Si atoms, will do to this system? Experimentally, it has been suggested that such geometrical deformation may be possible. In fact, the reported Si–Si bonds are 2.353 and 2.448 Å, respectively.[4] We decide to study such distortions in some detail, especially for the following reasons. For $M_2Ta_9S_6$ (M = Fe, Co), it has been shown that pairing of the M atoms in the center of trigonal-prismatical Ta_6 environment is a result of a Peierls distortion.[19] Obviously, such a distortion is a strong one, giving rise to two distinct M–M bonds, 2.88 and 3.70 Å for M = Fe and 2.90 and 3.67 Å for M = Co. In the compound under consideration, however, the situation is unclear. The two M–M bonds (M = Si) differ by only 0.095 Å, compared to 0.82 and 0.77 Å for M being Fe and Co, respectively, in $M_2Ta_9S_6$. With high standard deviations in the Si–Si bonds,[4] it is not apparent whether or not there is a real pairing occurring in this compound.

(19) Calhorda, M. J.; Hoffmann, R. *Inorg. Chem.* **1988**, *27*, 4679.

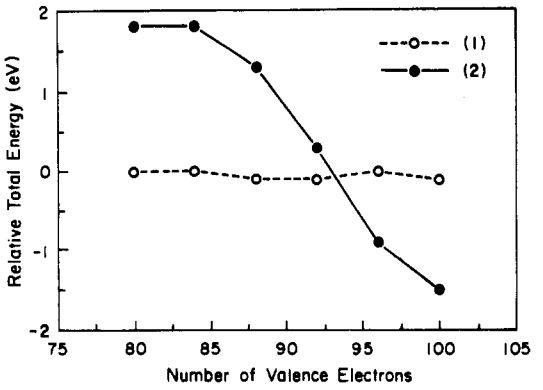

Figure 8. Relative average total energy change, $\Delta E_t = E_t$(undistorted) $- E_t$(distorted), as a function of the valence electron count. The solid line plots the result for the structure obtained after geometrical change in step 1 (pairing of silicons without any readjustment) and the dotted line, that obtained after step 2 (pairing with readjustments of tantalums, see text). The Ta_4Te_4Si chain (undistorted structure) is taken as the standard point (zero energy).

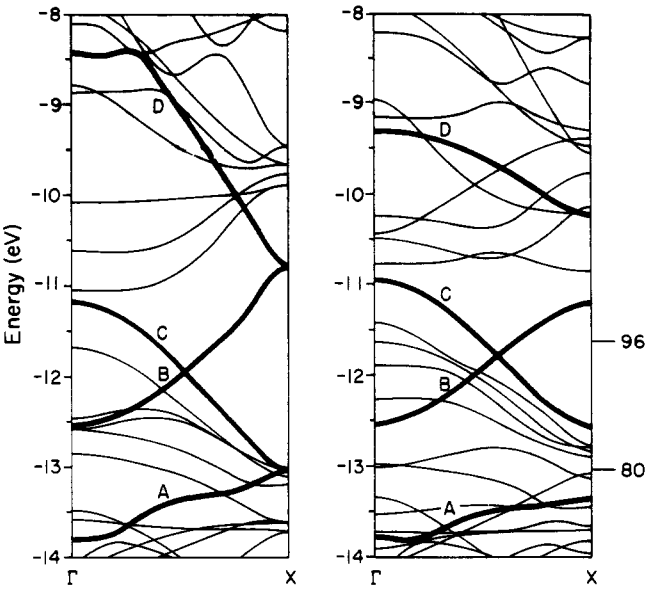

Figure 9. Band structure for the parent chain Ta_4Te_4Si and that after the change described in step 2. Bands that are affected mostly upon distortion are drawn with heavy lines and are labeled A, B, C, and D. Fermi levels for the electron fillings of 80 and 96 are indicated with horizontal bars for the distorted structure at right.

In a way similar to that described in ref 19, we do the following consecutively: (1) dimerize Si atoms and keep other parts of the chain unchanged, **18**; (2) stretch one Ta_4 square while contracting the other to adjust the Ta–Si distance as dimerization is taken place, **19**. Figure 8 compares the average total energy of the undistorted chain to the distorted ones generated from steps 1 and 2 versus the total valence electron count per unit cell (two formula units). The two curves indicate that the changes made in step 1 do not lead to any significant stabilization of the system. The curve that plots the energy difference between the parent structure and step 1 is extremely flat. With a system of 96 valence electrons as Ta_4Te_4Si, the calculated stabilization energy is only 0.1 eV. The average overlap populations calculated for step 1 (96 valence electrons per cell) differ negligibly from those obtained for the undistorted structure. Second, whether or not the chain favors the geometrical change made in step 2 depends on its valence electron count. Maximum stabilization is reached for an electron count of 80, whereas the system will be mostly destabilized for a valence electron count of 100. With 96 electrons, it is unlikely that Si atoms in Ta_4Te_4Si chain dimerize or pair up (along with expanding and contracting of the Ta squares) as do the Fe and Co atoms in $M_2Ta_9S_6$,[7] since such a deformation costs ~1.0 eV. To see how bands are altered during the course of distortion

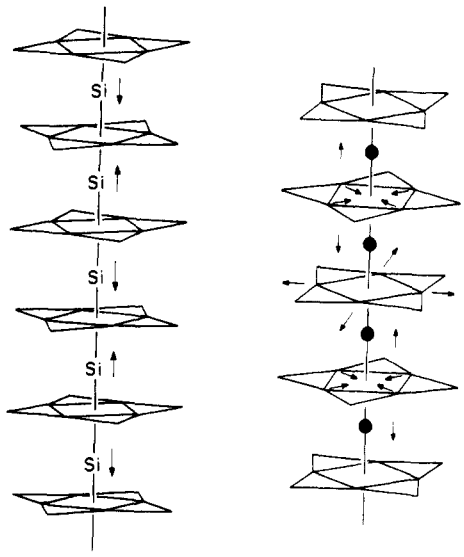

18 19

described in step 2, we plot out in Figure 9 the band structures of the chain before and after Si_2 pairing. In the latter case, the average bond lengths of Si–Si, Ta–Si, and Ta–Ta are kept same as in the former, 2.40, 2.59, and 3.26 Å. Other bond distances remain unchanged.

Bands that are affected significantly upon distortion are emphasized with heavy lines. The degeneracies at the zone edge in the undistorted structure (shown at the left of the figure) are a consequence of the symmetry due to the screw symmetry along the *c* axis. These degeneracies are destroyed after distortion (shown at the right of the figure), and a gap is created. Bands A and B are lowered, whereas bands C and D are lifted up in energy upon distortion. With 80 electrons, only A is filled, and great stabilization is obtained. When the electrons go up to 96, however, both B and C are partially filled. While filling B would stabilize the system, filling C has the opposite effect. The two compete, and the result is a net rise in the total energy. As more electrons are added to the system, one begins to fill D, which will make the structure even more unstable. This is reflected in Figure 8, where the curve moves down toward the more negative region as the number of electrons increases.

Replacing Si by Fe and Other Elements

The possibility of replacing Si atoms in the center of a metal cluster by other elements, such as the transition metal Fe (or Co) is not new. Corbett and co-workers have reported a series of zirconium clusters in which the encapsulated main-group elements (B, Al, C, and N) are replaced by the transition metals Mn, Fe, Co, and Ni.[20] In spite of many differences between the two groups of interstitial elements, some common features exist. The size and the electronegativity, for example, are both comparable for Si and Fe.[21]

The calculated overlap populations in the model Ta_4Te_4Fe structure mimic, surprisingly well, those of the parent structure Ta_4Te_4Si, except for the M–M bond (where M is the interstitial atom Si or Fe), which is certainly due to the different nature of the two types of bonding (Table II). Fragment (sublattice) analysis also indicates the same trend as exhibited in the Si compound. The most prominent change is found in the Fe–Fe bond, whose overlap population decreases from 0.262 in the sublattice $(Fe)_\infty$ to 0.115 in the composite Ta_4Te_4Fe. Both Ta–Ta and Ta–Ta′ bonds are also weakened (0.249 to 0.156 and 0.343 to 0.308, respectively). A strong attractive Ta–Fe interaction is indicated by its large positive overlap population, 0.262. Ta–Te bonding, both intra- and intersquare, shows almost no change.

Interactions between Ta and Fe are attributed greatly to their

(20) Hughbanks, T.; Rosenthal, G.; Corbett, J. D. *J. Am. Chem. Soc.* **1986**, *108*, 8289.
(21) Size: the atomic radii for Si and Fe atoms are 1.18 and 1.25 Å, respectively. Electronegativity: 1.9 for Si and 1.8 for Fe.

Table II. Overlap Population Values for the Ta_4Te_4Si and Ta_4Te_4Fe Structures

	OP	
	Ta_4Te_4Si	Ta_4Te_4Fe
M–M[a]	0.2804	0.1151
M–Ta	0.2702	0.2620
Ta–Ta	0.1562	0.1559
Ta–Ta′	0.2884	0.3084
Ta–Te	0.4366	0.4471
Ta–Te′	0.3965	0.3925

[a] M = Si or Fe.

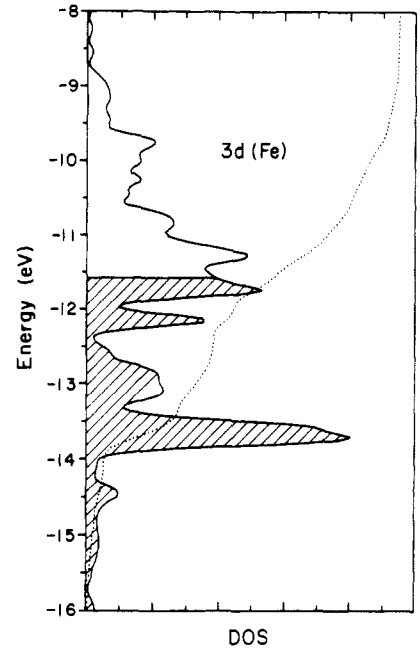

Figure 10. DOS projection of the Fe 3d orbitals in the model compound Ta_4Te_4Fe. The shaded area is filled with electrons. The dotted line gives the integration.

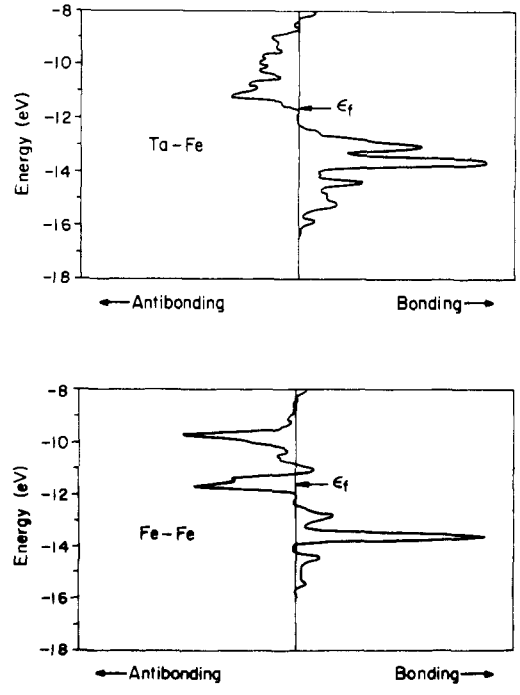

Figure 11. COOP curves of the model compound Ta_4Te_4Fe. That of the Ta–Fe bond is plotted at the top and that of the Fe–Fe bond is plotted at the bottom of the figure. The Fermi level is indicated with arrows.

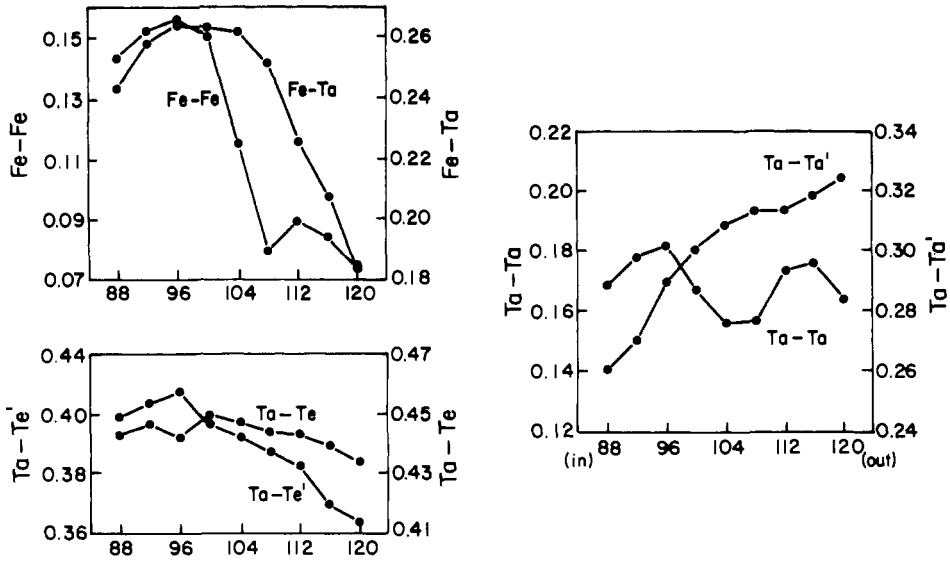

Figure 12. Crystal orbital overlap populations versus the valence electron count for the Ta_4Te_4Fe structure: Fe–Fe and Fe–Ta bonds (left, top); intra- and intersquare Ta–Te bonds (left, bottom); Ta–Ta, Ta–Ta′ bonds (right). The relative scale is the same in all plots.

atomic d orbitals. In a linear chain of iron atoms, the bonding is fairly localized. As illustrated in **20**, the dispersion of the σ-type

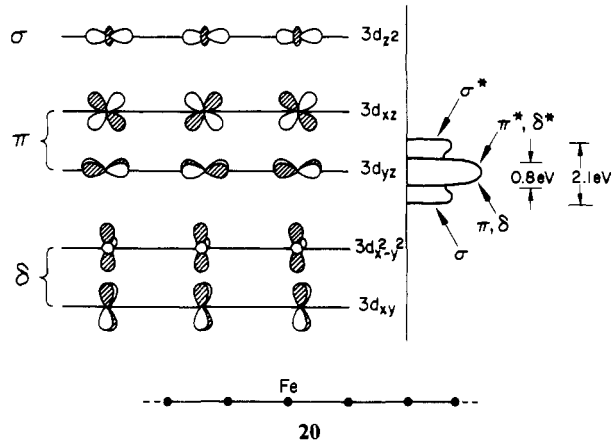

20

orbitals is about 2.1 eV, and is ~0.8 eV for the π and δ types. In the composite Ta_4Te_4Fe, the Fe 3d orbitals are much more spread out. The bandwidth, including up to 95% of the states, is more than 3 times wider (~6.5 eV). The contribution to the DOS of the Fe 3d orbitals in the composite system is plotted in Figure 10. It gives a pictorial view and shows how these states distribute in the energy region of −8.0 to −16.0 eV. The COOP curve plotted in Figure 11 shows that maximum Ta–Fe bonding would be reached for this model compound. Notice that all the Ta–Fe bonding states are occupied and the Fermi level is right at the bottom of the antibonding states.

The system should again be metallic, but this time, it is the Fe 3d orbitals that contribute largely to the conduction bands. A simple addition yields a distribution of 43.6%, 50.0%, and 6.4% to Fe (mostly 3d), Ta, and Te in an energy interval of 1 eV (−11.0 to −12.0 eV) around ϵ_F.

Along with the Ta–Fe COOP curve in Figure 11 is that of the Fe–Fe bond. One notices immediately that the antibonding states are also partially filled. This is of course an indication that one might think of oxidizing the Fe structure. However, one must not forget about other bonds: How will they respond to the removal of electrons from the system? To obtain a complete picture, we plot in Figure 12 all bond variations (in terms of overlap populations) versus valence electron count. With 104 electrons, i.e., a neutral chain of Ta_4Te_4Fe, the Fe–Ta bonding is very close to its maximum value, whereas the Fe–Fe bond is only about halfway to the maximum. While the intersquare Ta–Ta bond is approaching the top of its curve, the intrasquare Ta–Ta bond reaches the bottom of the curve. The overlap populations of the two Ta–Te bonds are not too far from their maximum. Removing electrons (oxidation) will result in a shift of the system to the left in each plot, and adding electrons (reduction) will result in a shift to the right. It is clear that both Ta–Fe and Fe–Fe bonding will be reduced in the system from reduction. The Ta–Te bonds will work in the same direction, but to a lesser extent. Oxidation, on the other hand, will probably lead to a net gain in bonding, at least over a small range of electron count from 104 to 96.

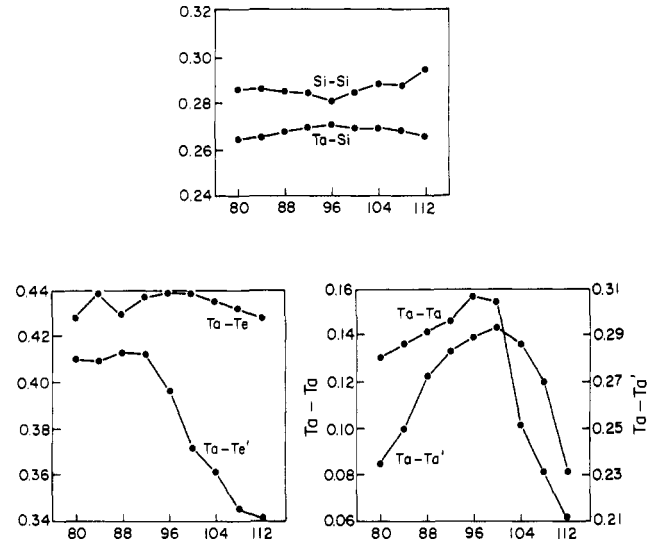

Figure 13. Crystal orbital overlap populations as a function of the valence electron count for the Ta_4Te_4Si chain: Si–Si and Ta–Si bonds (top); Ta–Te, Ta–Te′ bonds (bottom, left); Ta–Ta, Ta–Ta′ bonds (bottom, right).

The same plots are made for Ta_4Te_4Si in Figure 13 as a comparison. The situation is somewhat different there. Both the Ta–Si and Si–Si curves are flat. Therefore, they will be insensitive to a variation in the electron count. These bonds that do play a key role are the Ta–Ta bonds, both reaching a maximum overlap population at electron count of 96–100, and diminishing greatly as the electron count goes up or down. Another important factor comes from the Ta–Te′ bond, which is flat in the range of 80–92 electrons and decreases thereafter. Combining these factors, it seems that reduction is not favored for a system with 96 electrons, as in Ta_4Te_4Si. The tendency for oxidation is also less obvious as compared to the Fe structure.

Conclusions

Metal–metal bonding, both intra- and intersquare, is strong

Table III. Atomic Parameters Used in the Calculations

atom	orbital	H_{ii}, eV	ζ_1[a]	ζ_2[a]	c_1	c_2
Ta	6s	-10.1	2.28			
	6p	-6.86	2.24			
	5d	-12.12	4.76	1.94	0.6815	0.6815
Fe	4s	-8.40	1.90			
	4p	-5.00	1.90			
	3d	-12.2	5.35	2.00	0.5505	0.6815
Te	5s	-20.8	2.51			
	5p	-13.2	2.16			
Si	3s	-17.3	1.38			
	3p	-9.20	1.38			

[a] Exponent in the double ζ function for d orbitals.

in the Ta_4Te_4Si chain and is, by our calculations, to be attributed mostly to the Ta 5d orbitals. The Ta-Si bonding states are localized to a small energy interval. It is this bonding that greatly stabilizes the chain structure. The compound is expected to be metallic, with the conduction bands being largely made up of Ta 5d states. The staggered or antiprismatic form is more stable than the eclipsed one. While pairing of the interstitial atoms is in principle possible, it depends on the valence electron count. For a system with 96 electrons, as in Ta_4Te_4Si, the pairing distortion is not favored. An overlap population analysis indicates that replacing Si by Fe is quite feasible. The Fe compound thus obtained should again be conducting; the states around the Fermi level are now largely Fe 3d. Oxidation is more likely to take place than reduction, more so with the Fe compound than the Si compound.

Acknowledgment. We are grateful to the National Science Foundation for its generous support through Grant CHE 8912070. We thank Jane Jorgensen and Elisabeth Field for the drawings.

Appendix

The extended Hückel tight-binding method[8-9] is used throughout the paper. A summary of the atomic parameters is given in Table III. Atomic distances used in both structures, Ta_4Te_4M (M = Si, Fe), are 3.26 and 2.98 Å for the intra- and intersquare Ta-Ta bonds, 2.40 and 2.60 Å for the M-M and Ta-M bonds, and 2.85 Å (intrasquare) and 2.92 Å (intersquare) for the Ta-Te bonds. The k-point sets employed in the average property calculations are generated according to the Ramirez and Böhm method.[22]

(22) Ramirez, R.; Böhm, M. C. *Int. J. Quantum Chem.* **1986**, *30*, 391.

Contribution from the Department of Chemistry, Cornell University, Ithaca, New York 14853

Synthesis and Structure of Ta_4SiTe_4, a New Low-Dimensional Material

Michael E. Badding and F. J. DiSalvo*

Received November 21, 1989

The new infinite chain compound Ta_4SiTe_4 has been prepared by reaction of the elements at high temperature. The structure was refined in the orthorhombic space group *Pbam* with $Z = 4$ and lattice constants $a = 10.536$ (3), $b = 18.275$ (5), and $c = 4.799$ (1) Å to a final $R = 6.1\%$, $R_W = 8.2\%$. Ta_4SiTe_4 is a new structure type and represents a new class of compounds, Ta_4ZTe_4, with Z = Cr, Fe, Co, Ni, Al, or Si. The structure consists of Si-centered chains of antiprismatically stacked Ta squares that are edge bridged by Te.

Introduction

In the last few years, an abundant zirconium halide cluster chemistry has been discovered.[1-4] Many of the new zirconium phases are isoelectronic with and have structures related to well-known niobium halide cluster phases; the key difference is that they contain a heteroatom in the center of the zirconium octahedron. The heteroatom provides electrons necessary for the formation of a cluster phase in an otherwise electron-deficient system. A great variety of elements (Be, B, C, N, K, Al, Si, Ge, P, and 3d transition metals)[1-4] have been found to act as stabilizing heteroatoms in the zirconium halide system.

We considered whether, by analogy to the zirconium-niobium halides, new tantalum chalcogenides similiar to the remarkable Chevrel phases[5] of molybdenum could be synthesized by the addition of an appropriate stabilizing heteroatom. Initially, we focused on synthesizing carbon-centered tantalum chalogenide cluster phases using, for example, Ta_2S_2C as a precursor.[6] To date, we have been unable to synthesize such carbon-centered cluster phases. Subsequently, we investigated other Ta-Z-X systems (Z = stabilizing heteroatom; X = chalcogenide).

Here we report on the synthesis and structure of a new phase in the Ta-Si-Te system, Ta_4SiTe_4. This compound has a very unusual, low-dimensional structure based on Si-centered square-antiprismatic Ta_4Te_4 infinite chains. Weak Te-Te van der Waals interactions bond the chains together.

(1) Ziebarth, R. P.; Corbett, J. D. *J. Am. Chem. Soc.* **1985**, *107*, 4571.
(2) Smith, J. D.; Corbett, J. D. *J. Am. Chem. Soc.* **1986**, *108*, 1927.
(3) Hughbanks, T.; Rosenthal, G.; Corbett, J. D. *J. Am. Chem. Soc.* **1986**, *108*, 8289.
(4) Rosenthal, G.; Corbett, J. D. *Inorg. Chem.* **1987**, *27*, 53.
(5) Fischer, O. *Appl. Phys.* **1978**, *16*, 1.
(6) Ziebarth, R. P.; Vassiliou, J. K.; DiSalvo, F. J. *J. Less-Common Met.* **1989**, *156*, 207.

Synthesis

The title compound was first synthesized from a 1-g mixture of the elements with the molar ratio Ta:Si:Te = 2:1:2 in an evacuated quartz tube. $TeCl_4$ (10 mg) was included as a transport agent. The sample was heated in a furnace at 600 °C for 1 day and removed and placed in another furnace at 1150 °C for 4 days, followed by rapid quenching to room temperature. Large needlelike crystals with a metallic luster were formed. Microprobe analysis of the crystals indicated the presence of only tantalum, silicon, and tellurium. It was difficult to find a crystal of the appropriate size for single-crystal diffractometry as most crystals tended to grow very long (>1 mm) or very thin (<0.01 mm). Repeated attempts at growing single crystals have been most successful when both excess Te and small amounts of Cl are present. Plates of $TaTe_2$ are observed in the presence of excess Te. The crystal used in the structure determination below was taken from a reaction containing a 1-g mixture of the elements in the molar ratio Ta:Si:Te = 4:1:5 with 10 mg of $TeCl_4$; the previously mentioned heating schedule was used. After the structure was determined, a powder sample of Ta_4SiTe_4 was obtained quantitatively by heating a stoichiometric mixture of Ta (3N6), Si (5N), and Te (5N) in an evacuated quartz ampule to 1050 °C for 2 days. The powder diffraction pattern of this material matched the calculated pattern of Ta_4SiTe_4.

The crystals are very fragile and moderately air-sensitive; they decompose on sitting in air after a few days. Finely divided powders, on the other hand, often ignite on air exposure.

Structure Determination

Weissenberg photographs of a crystal mounted along the needle axis yielded approximate lattice constants and an orthorhombic unit cell symmetry. After many attempts, a 0.36 × 0.05 × 0.03 mm^3 crystal of adequate quality for single-crystal diffraction was found. Data were collected on a Syntex $P2_1$ diffractometer using Mo Kα radiation and a graphite monochromator. The crystal was enveloped in a stream of room-temperature nitrogen gas to prevent slow decomposition of the crystal in air. The history of three check reflections, taken every 50

0020-1669/90/1329-3952$02.50/0